Robotica (2016) volume 34, pp. 2546–2565. © Cambridge University Press 2015
doi:10.1017/S026357471500020X

A nonlinear trajectory tracking controller for mobile robots with velocity limitation via parameters regulation

Mario E. Serrano†, Sebastián A. Godoy†, Vicente A. Mut‡, Oscar A. Ortiz† and Gustavo J. E. Scaglia†§

†*Instituto de Ingeniería Química, Universidad Nacional de San Juan, Av. Libertador San Martín Oeste 1109, San Juan J5400ARL, Argentina*
‡*Instituto de Automática, Universidad Nacional de San Juan, Av. Libertador San Martín Oeste 1109, San Juan J5400ARL, Argentina*
§*Departamento de Automatización y Control Industrial, Facultad de Ingeniería Eléctrica y Electrónica, Escuela Politécnica Nacional, Quito, Ecuador*

(Accepted February 24, 2015. First published online: April 16, 2015)

SUMMARY
This paper addresses the problem of trajectory tracking control in mobile robots under velocity limitations. Following the results reported in ref. [1], the problem of trajectory tracking considering control actions constraint is focused and the zero convergence of the tracking errors is demonstrated. In this work, the original methodology is expanded considering a controller that depends not only on the position but also on the velocity. A simple scheme is obtained, which can be easily implemented in others controllers of the literature. Experimental results are presented and discussed, demonstrating the good performance of the controller.

KEYWORDS: Trajectory tracking control; Difference equations; Uncertainties; Nonlinear multivariable control; Mobile robot.

1. Introduction

Control problems involving mobile robots have recently attracted considerable attention in the control community. Mobile robots with a steering wheel (unicycle) or two independent drive wheels are examples with substantial engineering interest. Most wheeled mobile robots can be classified as nonholonomic mechanical systems. Controlling such systems is, however, deceptively simple. The challenge presented by these problems comes from the fact that a motion of a wheeled mobile robot in a plane possesses three-degrees of freedom (DOF); while it has to be controlled using only two control inputs under the nonholonomic constraint. In trajectory tracking problems, the objective is to find the control actions that make the mobile robot to reach a Cartesian position $(x_{\text{ref}}, y_{\text{ref}})$ with a pre-established orientation θ at each sampling period. These combined actions lead the mobile robot to track the desired trajectory.

This paper proposes a new approach to limit the control signals in a trajectory tracking of a unicycle-like mobile robot. In the literature it is common to find works that use explicit saturation functions, such as the hyperbolic tangent, to limit control signals.[2,3] In this work, a new control law based on linear algebra is proposed to achieve such limitation while keeping an efficient trajectory tracking controller operation. In addition, is presented a new scheme that allows to choose the controller parameters in order to accomplish the above objective. This algorithm is also applied to a controller previously developed by the authors.

Corresponding authors. E-mails: eserrano@fi.unsj.edu.ar, gscaglia@unsj.edu.ar, sgodoy@unsj.edu.ar, vmut@unsj.edu.ar, rortiz@unsj.edu.ar

https://doi.org/10.1017/S026357471500020X Published online by Cambridge University Press

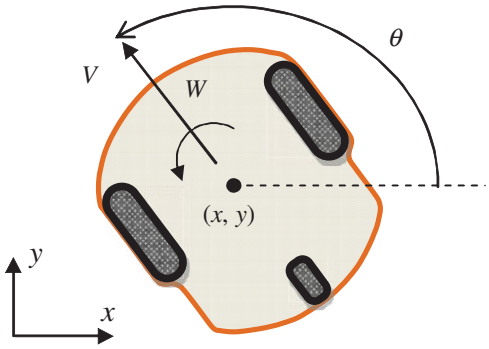


Fig. 1. Geometric description of the mobile robot.

In ref. [1], a novel trajectory tracking controller has been presented. The originality of this control approach is based on the application of linear algebra for trajectory tracking, where the control actions are obtained by solving a system of linear equations. The methodology developed for tracking the reference trajectory (x_{ref} and y_{ref}) is based on determining the trajectories of the remaining state variables, in order to the tracking error tends to zero. These states variables are determined by analyzing the conditions so that the system of linear equations has exact solution. To achieve this objective only two control variables are available: the linear velocity (V) and the angular velocity (W) of the robot (Fig. 1). This design technique has been applied successfully in several systems.[1,4–6]

Another typical problem, covered in the literature by other authors,[7,8] is the trajectory tracking with constraints in the control signals. In general, in a robot mobile system, the linear and angular velocities constraints prevent the mobile robot from slipping and actuators saturation. Nonlinear system theory has been employed to solve this problem in ref. [7]. In ref. [7], a saturation feedback controller (where the saturation constraints of the velocity inputs are incorporated into the controller design) is introduced. In ref. [8], a model-predictive trajectory tracking control applied to a mobile robot is presented. Linearized tracking-error dynamics is used to predict future system behavior and a control law is derived from a quadratic cost function penalizing the system tracking error and the control effort. In ref. [9], fuzzy rules are adopted to achieve such limitation, combining the heuristic knowledge of the problem, the sector nonlinearity approach and the inverse kinematic of the mobile platform.

This work is a continuation of refs. [1] and [10], and provides an accurate answer to the following challenging problem. The approaches here proposed consider the problem of designing controllers based on linear algebra for trajectory tracking ensuring that the values of the control actions do not exceed the maximum allowable. The main contributions of this work are a new control law and a new method for controllers' tuning.

The new controller proposed prevents the saturation of the actuators and ensures convergence to zero of tracking errors, this methodology is based on linear algebra and the trapezoidal approximation of the robots model. The trapezoidal approximation, here considered, includes the linear and angular references velocities in comparison of the control law presented in ref. [1].

The novel parameter assignment scheme presented in this work is based on the conditions that avoid the saturation of the control actions and on the conditions that ensure the convergence to zero of the tracking errors. In addition, a decremental reason of the controller parameters is defined in order to achieve such objective. This parameter assignment scheme is applied to the Euler based controller previously published by the authors and to the trapezoidal based controller here proposed.

The contributions, with respect to the previous works,[1,10] can be summarized as follows:

- Respect to ref. [1], a new control law is proposed. This law is based in the modification of the trapezoidal controller developed in ref. [1] (Eqs. (31) and (33)). Another important contribution respect to ref. [1] is a method for controller tuning that allows to choose the controller parameters (based on Euler approximation) proposed in Eq. (15) in ref. [1]. Furthermore, this work is included as an analysis of the controller parameters. The conditions so that the control actions do not exceed the maximum permitted and the tracking errors tend to zero arises from this analysis. The general

https://doi.org/10.1017/S026357471500020X Published online by Cambridge University Press

contribution proposed in this paper is achieving the limitation in the control actions while keeping an efficient trajectory tracking controller operation.
- Respect to ref. [10], the methodology is expanded considering a controller that depends on the reference position and reference velocities. In addition, a new scheme for the controller tuning is proposed. This approach is simple and requires a less calculation time compared to ref. [10]. Therefore, it is suitable for any microcontroller programming, because it is not necessary to solve an optimization problem at each sampling time. In addition, the convergence of the tracking error to zero for the trapezoidal controller here proposed is demonstrated in the Appendix.

It is noteworthy that due to the above mentioned characteristics of the controllers proposed in this paper, the computing power required to perform the mathematical operations is low. Therefore, it is possible to implement the algorithm in any controller with low computing capacity. Furthermore, the algorithm developed is easier to implement in a real system because the use of discrete equations allows direct adaptation to any computer system or programmable device running sequential instructions at a programmable clock speed. Thus, the main advantages of this approach are the simplicity of the controller and the use of discrete-time equations, simplifying its implementation on a computer system. The proof of the zero convergence of the tracking error is another main contribution of this work.

To develop and validate the proposed controller, the paper is hereinafter organized in seven sections. In Section 2, the kinematical model of the robot mobile is presented. The methodology of the Euler based controller design and the parameters analysis is shown in Section 3. In Section 4, a new control law based on the trapezoidal approximation is developed. The methodology for controller parameters selection is included in Section 5. Section 6 shows the experimental results and performance comparisons between the aforementioned controller.[10] Finally, Section 7 highlights some conclusions.

2. Kinematic Model of the Mobile Robot

This paper is a continuation of a previous work of the authors, in refs. [1] and [10]. A nonlinear kinematic model for a mobile robot will be used as shown in Fig. 1, represented by Eq. (1)

$$\begin{cases} \dot{x} = V\cos\theta \\ \dot{y} = V\sin\theta \\ \dot{\theta} = W \end{cases} \tag{1}$$

where, V is the linear velocity of the mobile robot, W is the angular velocity of the mobile robot, (x, y) is the Cartesian position, and θ is the mobile robot orientation. This model has been used in several recent papers such as.[5,11,12]

Then, the aim is to find the values of V and W so that the mobile robot follows a pre-established trajectory (x_{ref} and y_{ref}) with a minimum error. The values of $x(t)$, $y(t)$, $\theta(t)$, $V(t)$, and $W(t)$ at discrete time $t = nT_0$, where T_0 is the sampling time and $n \in \{0, 1, 2, \cdots\}$, will be denoted as x_n, y_n, θ_n, V_n, and W_n, respectively.

From Eq. (1), it follows

$$\begin{cases} x_{n+1} = x_n + \int_{nT_0}^{(n+1)T_0} V\cos\theta dt \\ y_{n+1} = y_n + \int_{nT_0}^{(n+1)T_0} V\sin\theta dt \\ \theta_{n+1} = \theta_n + \int_{nT_0}^{(n+1)T_0} W dt \end{cases} \tag{2}$$

In this work, the Euler and trapezoidal approximation are applied to the system of differential Eq. (1).

https://doi.org/10.1017/S026357471500020X Published online by Cambridge University Press

Remark 1: The value of the difference between the reference and real trajectory will be called tracking error. It is given by $e_{x,\,n} = x_{\mathrm{ref},n} - x_n$ and $e_{y,\,n} = y_{\mathrm{ref},_n} - y_n$. The tracking error is represented by $\|e_n\| = \sqrt{(e_{x,\,n}^2 + e_{y,\,n}^2)}$.

3. First Approach: Euler's Approximation

In this section, a control law previously published by the authors in ref. [1] is shown. Then the controller behavior is analyzed when its parameters vary.[10]

3.1. Controller design

Through the Euler's approximation of the kinematic model of the mobile robot in Eq. (1), the following set of equations is obtained:

$$\begin{cases} x_{n+1} = x_n + T_0 V_n \cos(\theta_n) \\ y_{n+1} = y_n + T_0 V_n \sin(\theta_n) \\ \theta_{n+1} = \theta_n + T_0 W_n \end{cases} \tag{3}$$

Equation (3) can be re-arranged as

$$\begin{bmatrix} x_{n+1} \\ y_{n+1} \\ \theta_{n+1} \end{bmatrix} = \begin{bmatrix} x_n \\ y_n \\ \theta_n \end{bmatrix} + T_0 \begin{bmatrix} \cos(\theta_n) & 0 \\ \sin(\theta_n) & 0 \\ 0 & 1 \end{bmatrix} \begin{bmatrix} V_n \\ W_n \end{bmatrix} \tag{4}$$

and the proposed controller is (see refs. [1] and [10], for details)

$$\begin{bmatrix} V_n \\ W_n \end{bmatrix} = \begin{bmatrix} \frac{x_{\mathrm{ref},n+1} - k_v(x_{\mathrm{ref},n} - x_n) - x_n}{T_0} \cos(\theta_{ez,n}) + \frac{y_{\mathrm{ref},n+1} - k_v(y_{\mathrm{ref},n} - y_n) - y_n}{T_0} \sin(\theta_{ez,n}) \\ \frac{\theta_{ez,n+1} - k_w(\theta_{ez,n} - \theta_n) - \theta_n}{T_0} \end{bmatrix} \tag{5}$$

where

$$\tan\theta_{ez,n} = \frac{\sin\theta_{ez,n}}{\cos\theta_{ez,n}} = \frac{\Delta_y}{\Delta_x} = \frac{y_{\mathrm{ref},_{n+1}} - k_v(y_{\mathrm{ref},_n} - y_n) - y_n}{x_{\mathrm{ref},_{n+1}} - k_v(x_{\mathrm{ref},_n} - x_n) - x_n}. \tag{6}$$

The reference trajectory is known, $x_{\mathrm{ref}}(t)$ and $y_{\mathrm{ref}}(t)$. The orientation θ_{ez} represents the necessary orientation to make the mobile robot tend to the reference trajectory; k_v and k_w are positive constants that permit to adjust the performance of the proposed control system. The controller parameters fulfilled $0 < k_v < 1$ and $0 < k_w < 1$ so as to the tracking errors tends to zero, see ref. [11] for details.

By inspection of (5) and (6), a proportional action (k_v and k_w) to the error is considered in the computation of the control inputs.

3.2. Analysis of Euler controller parameters

In this section, the performance of the system when the controller parameters vary is analyzed.[10]

Considering that the reference trajectory satisfy Eq. (2), hence

$$\begin{cases} x_{\mathrm{ref},_{n+1}} = x_{\mathrm{ref},_n} + T_0 V_{\mathrm{ref},_n} \cos(\theta_{\mathrm{ref},_n}) \\ y_{\mathrm{ref},_{n+1}} = y_{\mathrm{ref},_n} + T_0 V_{\mathrm{ref},_n} \sin(\theta_{\mathrm{ref},_n}) \\ \theta_{\mathrm{ref},_{n+1}} = \theta_{\mathrm{ref},_n} + T_0 W_{\mathrm{ref},_n} \end{cases} \tag{7}$$

From Eq. (7), the Eqs. (8) and (9) can be obtained. They represent the reference velocities at time n

$$V_{\mathrm{ref},_n} = \frac{x_{\mathrm{ref},_{n+1}} - x_{\mathrm{ref},_n}}{T_0} \cos(\theta_{\mathrm{ref},_n}) + \frac{y_{\mathrm{ref},_{n+1}} - y_{\mathrm{ref},_n}}{T_0} \sin(\theta_{\mathrm{ref},_n}) \tag{8}$$

$$W_{\mathrm{ref},_n} = \frac{\theta_{\mathrm{ref},_{n+1}} - \theta_{\mathrm{ref},_n}}{T_0}. \tag{9}$$

https://doi.org/10.1017/S026357471500020X Published online by Cambridge University Press

It is assumed that in each sampling time is fulfilled: $|V_{\text{ref},n}| < V_{\max}$ and $|W_{\text{ref},n}| < W_{\max}$, where, $V_{\max}$ and $W_{\max}$ are the maximum allowable speeds. These conditions are assumed in order to make it possible to follow the reference trajectory.

Now, robot velocities are analyzed when the controller parameters tends to one from the left side. If $k_v \to 1^-$ in Eq. (6)

$$\lim_{k_v \to 1^-} \theta_{ez,n} = \operatorname{atan} \frac{y_{\text{ref},n+1} - y_{\text{ref},n}}{x_{\text{ref},n+1} - x_{\text{ref},n}} = \theta_{\text{ref},n}. \tag{10}$$

Therefore, considering Eq. (5)

$$\lim_{\substack{k_v \to 1^- \\ k_w \to 1^-}} V_n = \frac{x_{\text{ref},n+1} - x_{\text{ref},n}}{T_0} \cos(\theta_{\text{ref},n}) + \frac{y_{\text{ref},n+1} - y_{\text{ref},n}}{T_0} \sin(\theta_{\text{ref},n}) = V_{\text{ref},n} \tag{11}$$

$$\lim_{\substack{k_v \to 1^- \\ k_w \to 1^-}} W_n = \frac{\theta_{\text{ref},n+1} - \theta_{\text{ref},n}}{T_0} = W_{\text{ref},n}. \tag{12}$$

As $|V_{\text{ref},n}| < V_{\max}$ and $|W_{\text{ref},n}| < W_{\max}$, from Eqs. (11) and (12) it can be seen that, when $k_v \to 1^-$ and $k_w \to 1^-$ then, $V_n \to V_{\text{ref},n}$ and $W_n \to W_{\text{ref},n}$; therefore $|V_n| < V_{\max}$ and $|W_n| < W_{\max}$. In ref. [10], the authors have demonstrated that the convergence to zero of the tracking error is ensured when the controllers parameters fulfills $0 < k_v < 1$ and $0 < k_w < 1$. Thus, the latter indicates, for the Euler based controller, that a parameter value below (but close) to one, guarantees the convergence to zero of the tracking error, and control actions do not exceed the allowable values.

If $k_v = 1$ and $k_w = 1$, verifies that

$$V_n = \frac{x_{\text{ref},n+1} - x_{\text{ref},n}}{T_0} \cos(\theta_{\text{ref},n}) + \frac{y_{\text{ref},n+1} - y_{\text{ref},n}}{T_0} \sin(\theta_{\text{ref},n}) = V_{\text{ref},n} \tag{13}$$

$$W_n = \frac{\theta_{\text{ref},n+1} - \theta_{\text{ref},n}}{T_0} = W_{\text{ref},n}. \tag{14}$$

The latter demonstrates that a value below but close to one of the controller parameters (k_v and k_w), makes the actual velocities of the robot tend to the velocities used to generate the reference trajectory, and that the tracking error converges to zero.

In Section 5, a novel methodology is proposed in order to solve the problem of selecting the k_v and k_w values.

4. Second Approach: (Trapezoidal-Type Integration Method)

In this section, the trapezoidal controller presented in ref. [1] is shown. In addition, its parameters analysis is performed. Then, by re-design of the trapezoidal controller a new control law is obtained. With this new controller, it is possible to avoid the saturation of the actuators in the mobile robot which is the purpose of this work.

4.1. Trapezoidal controller

A second controller proposed in ref. [1], is now presented. Through the trapezoidal approximation of the kinematic model of the mobile robot (Eq. (1)), the following set of equations can be obtained:

$$\begin{cases} x_{n+1} = x_n + \frac{T_0}{2} (V_n \cos\theta_n + V_{n+1} \cos\theta_{n+1}) \\ y_{n+1} = y_n + \frac{T_0}{2} (V_n \sin\theta_n + V_{n+1} \sin\theta_{n+1}) \\ \theta_{n+1} = \theta_n + \frac{T_0}{2} (W_n + W_{n+1}). \end{cases} \tag{15}$$

https://doi.org/10.1017/S026357471500020X Published online by Cambridge University Press

The Eq. (15) can be re-arranged as

$$\begin{bmatrix} \cos\theta_{n+1} & 0 \\ \sin\theta_{n+1} & 0 \\ 0 & 1 \end{bmatrix} \begin{bmatrix} V_{n+1} \\ W_{n+1} \end{bmatrix} = \begin{bmatrix} \frac{2}{T_0}(x_{n+1} - x_n) - V_n \cos\theta_n \\ \frac{2}{T_0}(y_{n+1} - y_n) - V_n \sin\theta_n \\ \frac{2}{T_0}(\theta_{n+1} - \theta_n) - W_n \end{bmatrix} \tag{16}$$

and the proposed controller is (see ref. [1] for details)

$$V_{n+1} = \left(\frac{2}{T_0}\Delta_x - V_n \cos\theta_n\right)\cos\theta_{ez,n+1} + \left(\frac{2}{T_0}\Delta_y - V_n \sin\theta_n\right)\sin\theta_{ez,n+1} W_{n+1} = \frac{2}{T_0}\Delta_\theta - W_n \tag{17}$$

where

$$\tan\theta_{ez,n+1} = \frac{\frac{2}{T_0}\left(y_{\text{ref},n+1} - k_v\left(y_{\text{ref},n} - y_n\right) - y_n\right) - V_n \sin\theta_n}{\frac{2}{T_0}\left(x_{\text{ref},n+1} - k_v\left(x_{\text{ref},n} - x_n\right) - x_n\right) - V_n \cos\theta_n} \tag{18}$$

and

$$\begin{aligned} \Delta_x &= x_{\text{ref},n+1} - k_v\left(x_{\text{ref},n} - x_n\right) - x_n \\ \Delta_y &= y_{\text{ref},n+1} - k_v\left(y_{\text{ref},n} - y_n\right) - y_n \\ \Delta_\theta &= \theta_{ez,n+1} - k_w\left(\theta_{ez,n} - \theta_n\right) - \theta_n. \end{aligned} \tag{19}$$

The reference trajectory ($x_{\text{ref}}(t)$ and $y_{\text{ref}}(t)$) is known. The orientation θ_{ez} represents the necessary orientation to make the mobile robot tend to reference trajectory; k_v and k_w are positive constants that allow adjust the performance of the proposed control law. The controller parameters fulfilled $0 < k_v < 1$ and $0 < k_w < 1$ to the tracking errors tends to zero, see ref. [11].

As can be seen in Eq. (17), (18), and (19), a proportional action (k_v and k_w) to the error is considered in the computation of the control inputs.

4.2. Analysis of trapezoidal controller's parameters

In this section, the performance of the system when the controller parameters vary is analyzed.

Considering that, the desired trajectory satisfy Eq. (15), thus

$$\begin{cases} x_{\text{ref},n+1} = x_{\text{ref},n} + \frac{T_0}{2}\left(V_{\text{ref},n}\cos\theta_{\text{ref},n} + V_{\text{ref},n+1}\cos\theta_{\text{ref},n+1}\right) \\ y_{\text{ref},n+1} = y_{\text{ref},n} + \frac{T_0}{2}\left(V_{\text{ref},n}\sin\theta_{\text{ref},n} + V_{\text{ref},n+1}\sin\theta_{\text{ref},n+1}\right) \\ \theta_{\text{ref},n+1} = \theta_{\text{ref},n} + \frac{T_0}{2}\left(W_{\text{ref},n} + W_{\text{ref},n+1}\right) \end{cases} \tag{20}$$

From Eq. (20)

$$\frac{\sin\theta_{\text{ref},n+1}}{\cos\theta_{\text{ref},n+1}} = \tan\theta_{\text{ref},n+1} = \frac{\frac{2}{T_0}\left(y_{\text{ref},n+1} - y_{\text{ref},n}\right) - V_{\text{ref},n}\sin\theta_{\text{ref},n}}{\frac{2}{T_0}\left(x_{\text{ref},n+1} - x_{\text{ref},n}\right) - V_{\text{ref},n}\cos\theta_{\text{ref},n}} \tag{21}$$

$$\begin{aligned} V_{\text{ref},n+1} = &\left(\frac{2}{T_0}\left(x_{\text{ref},n+1} - x_{\text{ref},n}\right) - V_{\text{ref},n}\cos\theta_{\text{ref},n}\right)\cos\theta_{\text{ref},n+1} \\ &+ \left(\frac{2}{T_0}\left(y_{\text{ref},n+1} - y_{\text{ref},n}\right) - V_{\text{ref},n}\sin\theta_{\text{ref},n}\right)\sin\theta_{\text{ref},n+1} \end{aligned} \tag{22}$$

$$W_{\text{ref},n+1} = \frac{2}{T_0}\left(\theta_{\text{ref},n+1} - \theta_{\text{ref},n}\right) - W_{\text{ref},n}. \tag{23}$$

https://doi.org/10.1017/S026357471500020X Published online by Cambridge University Press

The $V_{\text{ref},n+1}$ and $W_{\text{ref},n+1}$ represents the linear and angular velocities of the reference trajectory at the $n+1$ instant. The reference trajectory fulfills: $|V_{\text{ref},n+1}| < V_{\max}$ and $|W_{\text{ref},n+1}| < W_{\max}$.

Now, the controller performance is analyzed. First, the mobile orientation is evaluated, if $k_v \to 1^-$ in Eq. (18)

$$\lim_{k_v \to 1^-} \theta_{ez,n+1} = \lim_{k_v \to 1^-} \operatorname{atan} \frac{\frac{2}{T_0}\left(y_{\text{ref},n+1} - k_v\left(y_{\text{ref},n} - y_n\right) - y_n\right) - V_n \sin\theta_n}{\frac{2}{T_0}\left(x_{\text{ref},n+1} - k_v\left(x_{\text{ref},n} - x_n\right) - x_n\right) - V_n \cos\theta_n}$$
$$= \operatorname{atan} \frac{\frac{2}{T_0}\left(y_{\text{ref},n+1} - y_{\text{ref},n}\right) - V_n \sin\theta_n}{\frac{2}{T_0}\left(x_{\text{ref},n+1} - x_{\text{ref},n}\right) - V_n \cos\theta_n} \neq \theta_{\text{ref},n+1}. \tag{24}$$

Then, the linear and angular velocities are studied in Eq. (17), when $k_v \to 1^-$

$$\lim_{k_v \to 1^-} V_{n+1} = \left(\frac{2}{T_0}\left(x_{\text{ref},n+1} - x_{\text{ref},n}\right) - V_n \cos\theta_n\right) \cos\theta_{ez,n+1}$$
$$+ \left(\frac{2}{T_0}\left(y_{\text{ref},n+1} - y_{\text{ref},n}\right) - V_n \sin\theta_n\right) \sin\theta_{ez,n+1} \neq V_{\text{ref},n+1} \tag{25}$$

$$\lim_{k_w \to 1^-} W_{n+1} = \frac{2}{T_0}\left(\theta_{ez,n+1} - \theta_{ez,n}\right) - W_n \neq W_{\text{ref},n+1}. \tag{26}$$

Equations (25) and (26) show that a value below but close to one of the controller parameters (k_v and k_w), do not ensures that the actual velocities of the robot tends to the references velocities (V_{ref} and W_{ref}). Thus, is not possible with the control law proposed in ref. [1], ensure the trajectory tracking and avoid that the control actions exceed the allowable limits.

4.3. Trapezoidal controller re-designs: reference trapezoidal controller

In Section 4.2, the performance was shown of the controller proposed in ref. [1] when its parameters vary. It was demonstrated that: if k_v and k_w tend to 1 from left, the variables V_{n+1}, and W_{n+1} do not tend to reference values $V_{\text{ref},n+1}$, and $W_{\text{ref},n+1}$. Thus, is not possible, with the control law proposed in ref. [1], ensure the trajectory tracking and avoid that the control actions exceed the allowable limits. In order to provide a solution to the problem, we propose a new control law based on the re-design of the trapezoidal controller.

From Eq. (15), the control law to move from (x_n, y_n) to (x_{n+1}, y_{n+1}) can be derived. Considering Eq. (15) and replacing $[x_{n+1}, y_{n+1}]$ by the desired trajectory $[x_{d,n+1}, y_{d,n+1}]$, Eq. (27) is given

$$\begin{cases} V_{n+1}\cos\theta_{n+1} = \frac{2}{T_0}\left(x_{d,n+1} - x_n\right) - V_n \cos\theta_n \\ V_{n+1}\sin\theta_{n+1} = \frac{2}{T_0}\left(y_{d,n+1} - y_n\right) - V_n \sin\theta_n. \end{cases} \tag{27}$$

In order to avoid that the control actions exceeds the allowable limits and by inspection of Eqs. (25) and (26), we propose the following replacements:

$$\begin{array}{ccc} V_n\cos\theta_n & by & V_{\text{ref},n}\cos\theta_{\text{ref},n} \\ V_n\sin\theta_n & by & V_{\text{ref},n}\sin\theta_{\text{ref},n} \\ W_n & by & W_{ez,n} \end{array} \tag{28}$$

where

$$W_{ez,n} = \frac{\theta_{ez,n+1} - \theta_{ez,n}}{T_0}. \tag{29}$$

The orientation θ_{ez} is the robot's orientation value such that the tracking errors tend to zero, see Appendix. Analyzing the conditions for the system (16) has an exact solution, we define θ_{ez} in

https://doi.org/10.1017/S026357471500020X Published online by Cambridge University Press

Eq. (30). In order to get a single solution, from Eq. (27) the direction θ_{n+1} must be

$$\frac{\sin\theta_{n+1}}{\cos\theta_{n+1}} = \tan\theta_{n+1} = \frac{\frac{2}{T_0}\left(y_{d,n+1} - y_n\right) - V_{\text{ref},_n}\sin\theta_{\text{ref},_n}}{\frac{2}{T_0}\left(x_{d,n+1} - x_n\right) - V_{\text{ref},_n}\cos\theta_{\text{ref},_n}}. \tag{30}$$

The value of θ_{n+1} is thus defined, and will be called $\theta_{ez,n+1}$. As shown in Eq. (16), this is a three-equation system where linear and angular velocities are unknown; from Eqs. (16), (27), (28), (29), and (30), system (31) results

$$\begin{bmatrix} \cos\theta_{ez,n+1} & 0 \\ \sin\theta_{ez,n+1} & 0 \\ 0 & 1 \end{bmatrix} \begin{bmatrix} V_{n+1} \\ W_{n+1} \end{bmatrix} = \begin{bmatrix} \frac{2}{T_0}\left(x_{d,n+1} - x_n\right) - V_{\text{ref},_n}\cos\theta_{\text{ref},_n} \\ \frac{2}{T_0}\left(y_{d,n+1} - y_n\right) - V_{\text{ref},_n}\sin\theta_{\text{ref},_n} \\ \frac{2}{T_0}\left(\theta_{d,n+1} - \theta_n\right) - W_{ez,n} \end{bmatrix}. \tag{31}$$

At time n, the mobile is at $[x_n, y_n]$, in order to get a smooth trajectory, the desirable next state, $[x_{d,n+1}, y_{d,n+1}]$, is not necessarily the new reference state value. This state vector ($[x_{d,n+1}, y_{d,n+1}]$) is replaced according to Eq. (32), assuming an proportional approach to the error. Furthermore, in Eq. (31) the orientation $\theta_{d,n+1}$ will be replaced by a proportional term to the error between $\theta_{ez,n}$ and θ_n, in order to get a smooth trajectory.[1] With this considerations, Eq. (32) is defined

$$\begin{aligned} x_{d,n+1} &= x_{\text{ref},_{n+1}} - k_v\left(x_{\text{ref},_n} - x_n\right) \\ y_{d,n+1} &= y_{\text{ref},_{n+1}} - k_v\left(y_{\text{ref},_n} - y_n\right) \\ \theta_{d,n+1} &= \theta_{ez,n+1} - k_w\left(\theta_{ez,n} - \theta_n\right). \end{aligned} \tag{32}$$

Where the controller parameters fulfills $0 < k_v < 1$ and $0 < k_w < 1$, in order to make the tracking errors tend to zero, (see Appendix). Note that

- If $k_v = 0$, ($x_{d,n+1} = x_{\text{ref},_{n+1}}$), the goal is to reach the reference trajectory in one step.
- If $k_v = 1$, the error will remain constant, ($x_{d,n+1} - x_n = x_{\text{ref},_{n+1}} - x_{\text{ref},_n}$).

The same analysis can be applied to $y_{d,n+1}$ and $\theta_{d,n+1}$. Next, we define

$$\begin{aligned} \Delta_x &= x_{\text{ref},_{n+1}} - k_v\left(x_{\text{ref},_n} - x_n\right) - x_n \\ \Delta_y &= y_{\text{ref},_{n+1}} - k_v\left(y_{\text{ref},_n} - y_n\right) - y_n \\ \Delta_\theta &= \theta_{ez,n+1} - k_w\left(\theta_{ez,n} - \theta_n\right) - \theta_n \end{aligned} \tag{33}$$

$$\begin{bmatrix} \cos\theta_{ez,n+1} & 0 \\ \sin\theta_{ez,n+1} & 0 \\ 0 & 1 \end{bmatrix} \begin{bmatrix} V_{n+1} \\ W_{n+1} \end{bmatrix} = \begin{bmatrix} \frac{2}{T_0}\Delta_x - V_{\text{ref},_n}\cos\theta_{\text{ref},_n} \\ \frac{2}{T_0}\Delta_y - V_{\text{ref},_n}\sin\theta_{\text{ref},_n} \\ \frac{2}{T_0}\Delta_\theta - W_{ez,n} \end{bmatrix}. \tag{34}$$

The system (34) is of the type $Au = b$, with more equations than unknowns. Its solution by least squares can be obtained by solving the normal equations,[13] $\boldsymbol{A}^{\mathrm{T}}\boldsymbol{A}u = \boldsymbol{A}^{\mathrm{T}}\boldsymbol{b}$, and thence, the proposed controller is

$$\begin{aligned} V_{n+1} &= \left(\frac{2}{T_0}\Delta_x - V_{\text{ref},_n}\cos\theta_{\text{ref},_n}\right)\cos\theta_{ez,n+1} + \left(\frac{2}{T_0}\Delta_y - V_{\text{ref},_n}\sin\theta_{\text{ref},_n}\right)\sin\theta_{ez,n+1} \\ W_{n+1} &= \frac{2}{T_0}\Delta_\theta - W_{ez,n} \end{aligned} \tag{35}$$

Proof 1. If the system behavior is ruled by Eq. (15) and the controller is designed by Eqs. (30), (33), and (35), then $e_n \to 0, n \to \infty$ when trajectory tracking problems are considered and the controller parameters fulfill $0 < k_v < 1$ and $0 < k_w < 1$.

https://doi.org/10.1017/S026357471500020X Published online by Cambridge University Press

The Proof 1 analysis is shown in Appendix.

4.4. Analysis of reference trapezoidal controller's parameters

Now, the performance of the controller proposed in Section 4.3 when its parameters vary is discussed.

Considering that the desired trajectory satisfies Eq. (15), then Eqs. (21), (22), and (23) are fulfilled. Here also, $\theta_{\text{ref},n+1}$, $V_{\text{ref},n+1}$, and $W_{\text{ref},n+1}$ are the mobile robot orientation, linear and angular velocities of the reference trajectory, and the reference trajectory fulfills: $|V_{\text{ref},n+1}| < V_{\max}$ and $|W_{\text{ref},n+1}| < W_{\max}$.

Next, the trapezoidal controller performance is analyzed. First, the mobile orientation is evaluated in Eq. (30), when $k_v \to 1$.

$$\begin{aligned}\lim_{k_v\to 1^-}\theta_{ez,n+1} &= \lim_{k_v\to 1^-}\operatorname{atan}\frac{\frac{2}{T_0}\left(y_{\text{ref},n+1}-k_v\left(y_{\text{ref},n}-y_n\right)-y_n\right)-V_{\text{ref},n}\sin\theta_{\text{ref},n}}{\frac{2}{T_0}\left(x_{\text{ref},n+1}-k_v\left(x_{\text{ref},n}-x_n\right)-x_n\right)-V_{\text{ref},n}\cos\theta_{\text{ref},n}}\\ &= \operatorname{atan}\frac{\frac{2}{T_0}\left(y_{\text{ref},n+1}-y_{\text{ref},n}\right)-V_{\text{ref},n}\sin\theta_{\text{ref},n}}{\frac{2}{T_0}\left(x_{\text{ref},n+1}-x_{\text{ref},n}\right)-V_{\text{ref},n}\cos\theta_{\text{ref},n}}\end{aligned} \tag{36}$$

By inspection of Eqs. (21) and (30), when $k_v \to 1^-$, Eq. (37) is given. As can be seen, $\theta_{ez,n+1} \to \theta_{\text{ref},n+1}$.

$$\lim_{k_v\to 1^-}\theta_{ez,n+1} = \theta_{\text{ref},n+1}. \tag{37}$$

Next, the linear velocity (V) is analyzed. From Eqs. (35) and (37)

$$\begin{aligned}\lim_{k_v\to 1^-}V_{n+1} = &\left(\frac{2}{T_0}\left(x_{\text{ref},n+1}-x_{\text{ref},n}\right)-V_{\text{ref},n}\cos\theta_{\text{ref},n}\right)\cos\theta_{\text{ref},n+1}\\ &+\left(\frac{2}{T_0}\left(y_{\text{ref},n+1}-y_{\text{ref},n}\right)-V_{\text{ref},n}\sin\theta_{\text{ref},n}\right)\sin\theta_{\text{ref},n+1}\end{aligned} \tag{38}$$

By comparison of Eqs. (22) and (38), when $k_v \to 1^-$, Eq. (39) is given.

$$\lim_{k_v\to 1^-}V_{n+1} = V_{\text{ref},n+1}. \tag{39}$$

Finally, the angular velocity (W) is evaluated. From Eq. (35)

$$\lim_{k_w\to 1^-}W_{n+1} = \frac{2}{T_0}\left(\theta_{\text{ref},n+1}-\theta_{\text{ref},n}\right)-W_{ez,n} = \frac{2}{T_0}\left(\theta_{\text{ref},n+1}-\theta_{\text{ref},n}\right)-\frac{\theta_{ez,n+1}-\theta_{ez,n}}{T_0}. \tag{40}$$

Considering Eq. (37) and replacing in Eq. (40)

$$\lim_{\substack{k_v\to 1^-\\ k_w\to 1^-}}W_{n+1} = \frac{2}{T_0}\left(\theta_{\text{ref},n+1}-\theta_{\text{ref},n}\right)-\frac{\theta_{\text{ref},n+1}-\theta_{\text{ref},n}}{T_0} = \frac{2}{T_0}\left(\theta_{\text{ref},n+1}-\theta_{\text{ref},n}\right)-W_{\text{ref},n}. \tag{41}$$

According to Eqs. (23) and (41), when $k_w \to 1^-$, the Eq. (42) is given.

$$\lim_{\substack{k_v\to 1^-\\ k_w\to 1^-}}W_{n+1} = W_{\text{ref},n+1}. \tag{42}$$

From Eqs. (38) and (41), when $k_v \to 1^-$ and $k_w \to 1^-$ then, $V_n \to V_{\text{ref},n}$ and $W_n \to W_{\text{ref},n}$; therefore, $|V_n| < V_{\max}$ and $|W_n| < W_{\max}$. The latter demonstrates that a value below but close to one of the parameters (k_v and k_w), make that the actual velocities of the robot tend to the velocities used to generate the trajectory and the tracking error converges to zero. Thus, the aim of this work can be accomplish.

In the next section is shown a new algorithm to select the controller parameters (k_v and k_w) in order to the tracking error tends to zero, and the control actions do not exceed the allowable limits.

https://doi.org/10.1017/S026357471500020X Published online by Cambridge University Press

Remark 2: The results obtained in this work fulfill with Brockett's theorem.[14]

5. Election of Controller Parameters by Delta Method

In this section, we propose an algorithm to find in each sampling time the controller parameters, such that the tracking errors tend to zero and the control actions do not exceed allowable limits.

In Sections 3.2 and 4.4, it was shown for the Euler controller (presented in Section 3.1) and the trapezoidal controller (proposed in Section 4.3) that: if k_v and k_w tend to one from the left, then, $V_n \to V_{\text{ref},n}$ and $W_n \to W_{\text{ref},n}$; therefore $|V_n| < V_{\max}$ and $|W_n| < W_{\max}$. With this in mind, an algorithm that is running on each sample time is proposed. The controller parameters are initialized at each sampling time with values close to one ($k_{v\max}$ and $k_{w\max}$), these values result in control actions that do not exceed the maximum allowable values. Then, its parameters are decreased according to the scheme proposed in Fig. (2), where δ is the value of decreasing reason. The algorithm ends when control actions are less than the allowed maximum speeds or the controller parameters take their minimum values ($k_{v\min}$ and $k_{w\min}$).

Remark 3: The values of $k_{v\min}$, $k_{w\min}$, $k_{v\max}$, and $k_{w\max}$ are determined by empirical tests in the same way as in ref. [10]. In the experimentation, these values are set as 0.942, 0.942, 0.99, and 0.99 respectively.

It is important to remark that the algorithm proposed in Fig. (2) is running in each sample time. By analyzing Fig. (2), it can be seen that the ending conditions of the algorithm are as follows:

- Control actions reached the value of the permitted maximum speeds.
- The controller parameters take their minimum values allowed ($k_{v\min}$ and $k_{w\min}$).

These two conditions ensure that always it will be find a feasible solution to implement in each sample time. Also ensure that tracking errors tend to zero, since the parameters of the controller always fulfill $0 < k_v < 1$ and $0 < k_w < 1$ (see Appendix).

6. Experimental Results

In this section, four experiments are reported to demonstrate the operation of the proposed controllers. Furthermore, the performance of the proposed controller is compared with the performance of the controller proposed in ref. [10], where a nonlinear programming technique is used to limit the control actions.

The experiments are performed using a PIONEER 3AT mobile robot. The PIONEER 3AT mobile robot includes an estimation system based on odometric positioning system. Updating through external sensors is necessary. This problem is separated from the strategy of trajectory tracking and it is not considered in this paper.[15,16] The PIONEER 3AT has a PID velocity controller used to maintain the velocities of the mobile robot at the desired value. Figure 3 shows the PIONEER 3AT and the laboratory facilities where the experiments were carried out.

Next, several experiments are shown to evaluate the performance of the proposed controllers in different scenarios. In the first place, the behavior of the proposed controller in Section 3.1 (called C1 in the sequel) and the proposed controller in Section 4.4 (called C2 in the sequel) is proved. Both controllers use the algorithm proposed in Section 5 to calculate the control actions. Secondly, an experiment is performed in order to compare the approaches proposed in this work (C1 and C2) with a controller recently developed in the literature in ref. [10] (C3 in the sequel). Finally, the controllers' performance when the sampling time is decreased is analyzed.

In order to compare the controllers performances, the integrated squared error (ISE) is used.[17,18] An idea widely used in the literature is to consider the cost incurred by the error. Let Φ be a desired trajectory, where # Φ is the number of points of such trajectory. Let $C_x^{\Phi} = T_0 . \sum_{i=0}^{\#\Phi} (x_{(i)} - x_{\text{ref}(i)})^2$ the ISE in the x-coordinate; and $C_y^{\Phi} = T_0 . \sum_{i=0}^{\#\Phi} (y_{(i)} - y_{\text{ref}(i)})^2$ the integrated quadratic error in the y-coordinate, as proposed in refs. [17, 18]. Then, the cost function can be represented for the combination of both, the ISE in x-coordinate and the y-coordinate as shown in Eq. (43)

$$C^{\Phi} = C_x^{\Phi} + C_y^{\Phi} = T_0 . \sum_{i=0}^{\#\Phi} \left((x_{(i)} - x_{\text{ref}(i)})^2 + (y_{(i)} - y_{\text{ref}(i)})^2 \right). \tag{43}$$

https://doi.org/10.1017/S026357471500020X Published online by Cambridge University Press

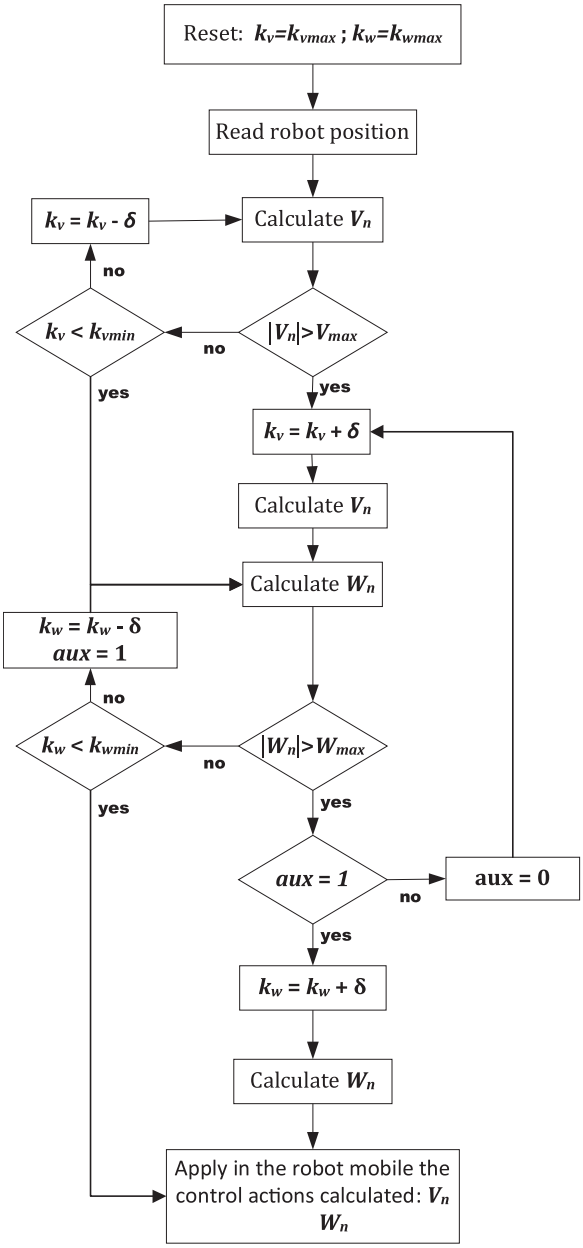


Fig. 2. Flow chart of delta method.

Remark 4: In the implementation of the proposed controllers in this paper, Eqs. (21) and (30), which allow to find $\theta_{\text{ref},n+1}$, are solved by the functions *atan2* and *unwrap* of MatLab®. The function *atan2* is the arctangent function with two arguments. The purpose of using two arguments instead of one is to gather information on the signs of the inputs in order to return the appropriate quadrant of the computed angle. The function *unwrap* corrects the radian phase angles in a vector. For details of these functions, see the Help of MatLab®.

6.1. Curvature test: circle-shaped trajectories

The first test carried out is a curvature test recommended in ref. [19], in which the controllers performance using different circle-shaped trajectories are probed. Three circle-trajectories were used in this work, with different radius. The internal trajectory has a radius of $r = 1.5$ m, the middle $r = 2.5$ m, and the last one $r = 3.5$ m. The initial position of the robot is the origin of the coordinate

https://doi.org/10.1017/S026357471500020X Published online by Cambridge University Press



Fig. 3. PIONEER 3AT and the laboratory.

system and the trajectory begins in the position $(x_{ref}, y_{ref}) = (1.5\text{ m}, 0\text{ m})$ and the sample time is set as $T_0 = 0.1$ s.

The reference trajectory and the results of the controllers are shown in Fig. (4a). As can be seen, all controllers reach and follow the desired trajectory. Figure (4b) shows the plots of the tracking error in the x-coordinate and y-coordinate according to each controller used in the test. The Euler based controller, proposed in Section 3.1 named C1, presents a similar performance that C2 (our approach with trapezoidal approximation), but the lowest cost is obtained by C2, as can be seen in Fig. (4f). The control actions are shown in Fig. (4c). These actions make the mobile robot follow the desired trajectory, without exceeding the maximum values of linear and angular velocities. The values of the controller parameters at each sampling time are shown in Fig. (4d). The controller parameters changes to ensure that the tracking errors tend to zero and the control actions do not exceed the maximum allowed. The processing timed for each controller is show in Fig. (4e): in general, C1 and C2 present a similar performance. Nevertheless, the trapezoidal based approach (C2) has more processing time in some sampling periods (blue-peaks) compared with C1. It is because C2 includes more information of the reference trajectory (θ_{ref}, V_{ref}, W_{ref}) in each sample time, then, more time is required to calculate the control actions. However, in the two controllers C1 and C2, the processing time is less than the sampling period for the entire trajectory.

6.2. Controller comparison

To test the advantages and drawbacks of our proposal, an experimental evaluation was carried out. For this reason, one controller previously published in the scientific literature was implemented for comparison on the mobile robot Pioneer 3AT. The controllers implemented for comparison are the following:

- Controller show in Section 3.1, C1 in the sequel (based on Euler approximation). In order to limit the control actions, the scheme proposed in Section 5 was applied.
- The controller developed in Section 4.3, C2 in the sequel (based on trapezoidal approximation). To limit the control actions the scheme proposed in Section 5 was used.
- A nonlinear trajectory tracking strategy developed by,[10] C3 in the sequel. This approach proposes nonlinear programming techniques to limit the control action.

The design details of the controller can be found in its respective references, and only the experimental results without a theoretical analysis of the controller's properties are shown here. For those,[10] offer a deep insight into the controller design.

Two tests with different trajectory references were performed to compare the controllers' behavior. First, a sinusoidal trajectory is generated with $V_{\text{ref}} = 0.5$ m/s, the initial position of the robot is at the

https://doi.org/10.1017/S026357471500020X Published online by Cambridge University Press

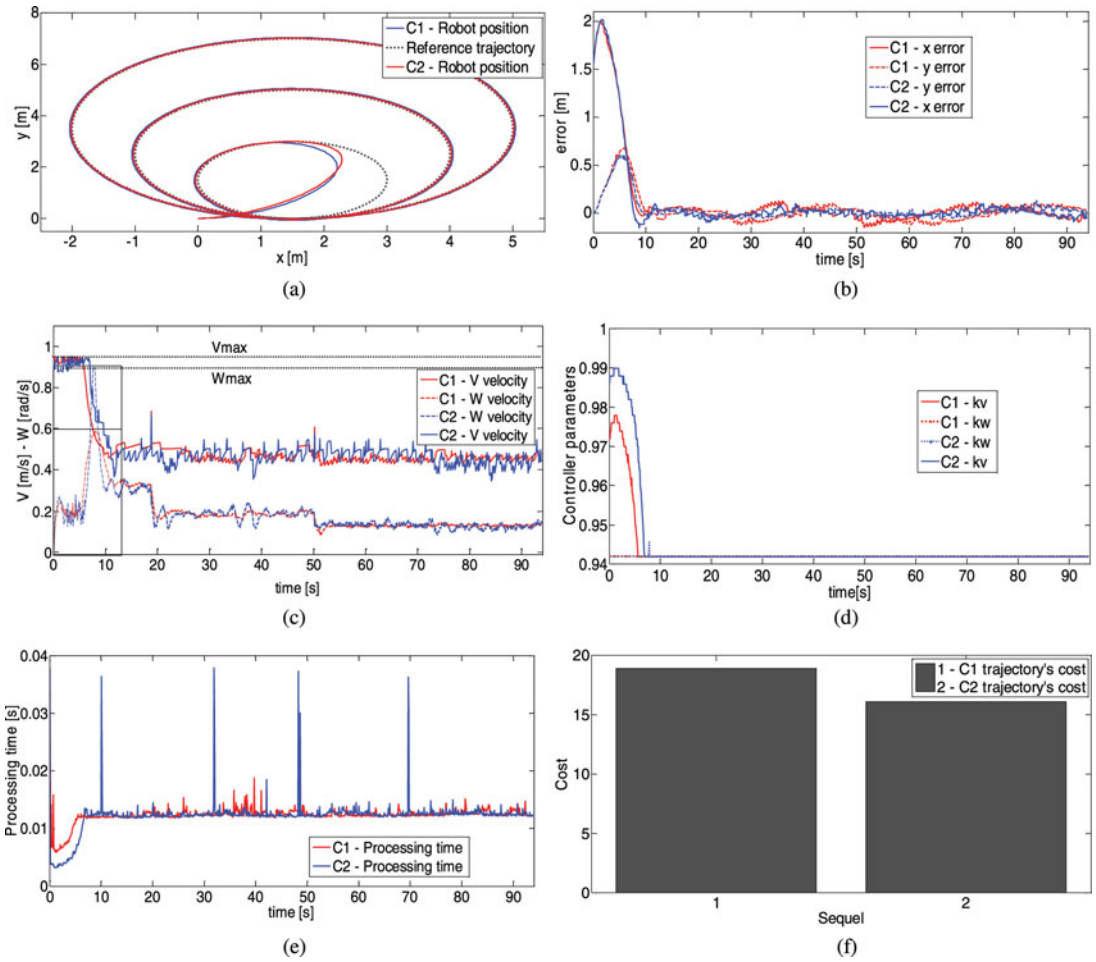


Fig. 4. (a) Tracking trajectory of the mobile robot; (b) Tracking errors vs. time; (c) Control actions vs. time; (d) Controller parameters vs. time; (e) Processing time vs. time; (f) Trajectories' cost.

system origin and the trajectory begins in the position $(x_{\text{ref}}, y_{\text{ref}}) = (1\text{ m}, 1\text{ m})$. The sample time used is $T_0 = 0.1$ s.

Figure (5a) shows the tracking trajectory of the controllers C1, C2, and C3. As can be seen, the controllers reach and follow the desired trajectory without unexpected oscillations. Figure (5d) shows that C2 is the controller with the lowest error. Figure (5b) shows the absolute values of the tracking errors for the *x-coordinate* and *y-coordinate* respectively. By inspection of the figures, the tracking error of C2 is the lowest and present a better performance against unwanted disturbances compared with C1 and C2. The processing time for the three controllers is show in Fig. (5c). As can be seen, the processing time of C1 and C2 is lower than C3's processing time. This is due to C1 and C2 do not need to perform any optimization to calculate the control actions in each sampling period.

In order to test the limits of our formulation, the second test carried out is a square trajectory, as recommended by ref. [19]. This strategy can be used in applications such as obstacle avoidance and contour-following. So if the danger of collision is large, the trajectory to be followed by the robot is modified abruptly and the robot must follow that path to avoid collision. In several applications, the desired trajectory to be followed by the robot is usually re-planned. Thus, the controller performance when the trajectory changes abruptly will be analyzed. The square reference trajectory is generated with constant linear velocity of $V = 0.3$ m/s. The initial position of the robot is at the system origin and the trajectory begins in the position $(x_{\text{ref}(0)}, y_{\text{ref}(0)}) = (2\text{ m}, 1\text{ m})$. The sample time used is $T_0 = 0.1$ s.

Figure (6) shows the results of the implementation. By inspection of Fig. (6a), all controllers reach and follow the reference trajectory. However, for the square trajectory test, C2 shows the lowest error

https://doi.org/10.1017/S026357471500020X Published online by Cambridge University Press

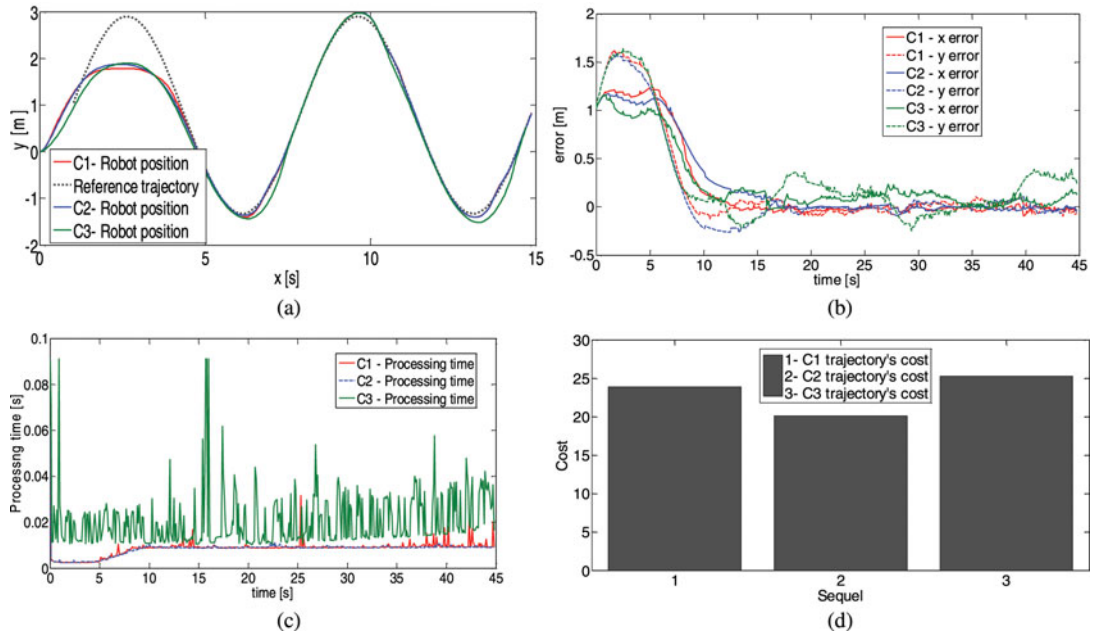


Fig. 5. (a) Tracking trajectory of the mobile robot; (b) Tracking errors vs. time; (c) Processing time vs. time; (d) Cost of the trajectory tracking.

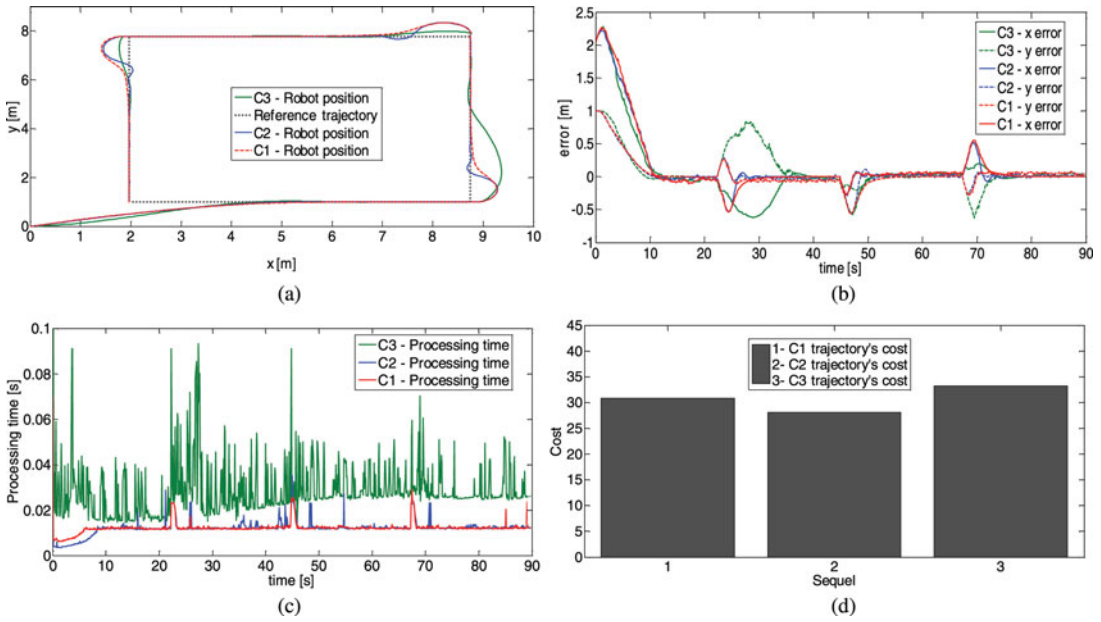


Fig. 6. (a) Tracking trajectory of the mobile robot; (b) Tracking error vs. time; (c) Processing time vs. time; (d) Cost of the trajectory tracking.

cost (as defined in Eq. (43)) when compared to the rest of the controllers (Fig. (6d)). This result can also be observed in Fig. (6b), which show the tracking errors in the x and y coordinate. Furthermore, the controllers C1 and C2 have a quicker response to an abrupt change in the reference trajectory as can be seen in Figs. (6a) and (6b). In this test, it is also verified that the processing time of C1 and C2 is lower than the C3's processing time, as shown in Fig. (6c).

6.3. Experimental results decreasing the sample time

In order to expand the analysis and to enhance the controller performance, the sampling time is decreased to: $T_0 = 0.05$ s, as recommended.[11] In order to verify that proposal, here we used the

https://doi.org/10.1017/S026357471500020X Published online by Cambridge University Press

Table I. Summary of the costs obtained by the controllers.

Sampling time/controllers	**Trajectory cost for C1**	**Trajectory cost for C2**
$T_0 = 0.1s$	$C^{\Phi} = 18.935$	$C^{\Phi} = 16.185$
$T_0 = 0.05s$	$C^{\Phi} = 16.297$	$C^{\Phi} = 15.043$

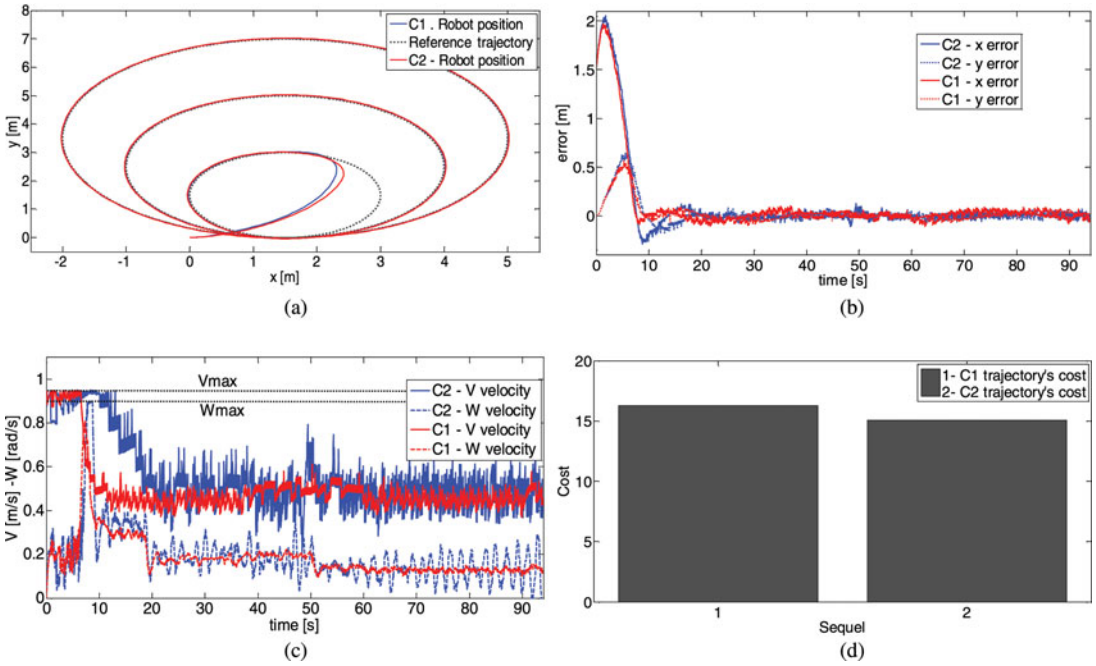


Fig. 7. (a) Tracking trajectory of the mobile robot; (b) Tracking error vs. time; (c) Control actions vs. time; (d) Cost of the trajectory tracking.

Table II. Maximum tracking error obtained by the controllers..

Sampling time/controllers	**Maximum tracking error for C1**	**Maximum tracking error for C2**
$T_0 = 0.1s$	$e_{\max} = 0.1521$m	$e_{\max} = 0.1287$m
$T_0 = 0.05s$	$e_{\max} = 0.1140$m	$e_{\max} = 0.0963$m

same conditions and desired trajectory reported in test of Section 6.1 but using a sampling time $T_0 = 0.05$ s.

The experimental results of this test are shown in Fig. (7). Figure (7b) shows the evolution of the tracking errors for the three curvatures presented in Fig. (7a). When comparing Figs. (4b) and (7b), it is observed that the tracking errors have considerably decreased. The costs obtained in this test and the obtained in Section 6.1 are shown in Table I. Analyzing the Table I, the cost obtained with $T_0 = 0.05$ s is 10% less compared with $T_0 = 0.1$ s. This, can also be seen when comparing Figs. (4f) and (7d), where the trajectory cost for the two controller is shown with $T_0 = 0.1$ s and $T_0 = 0.05$ s, respectively.

Based in an experimental analysis, decreasing sample time an error reduction is observed; this reduction obeys mainly to the additive disturbance and the fact that the error from unmodeled dynamics is corrected faster, keeping errors from kinematic considerations very small, as pointed in ref. [11]. Figure (7c) shows that the control actions do not exceed the maximum allowed values and remain close to $V_{\text{ref},n}$ and $W_{\text{ref},n}$.

The maximum tracking errors when the robot follows the reference trajectory are shown in Table II.

https://doi.org/10.1017/S026357471500020X Published online by Cambridge University Press

7. Conclusions

This paper proposes and validates a new technique for trajectory tracking in mobile robots limiting the control signals. One of the most significant contributions of this work involves the application of a method to find the parameters of the controller developed by ref. [1]. This method can be used to find values of the control actions that do not exceed the actuators saturation limits and forces the tracking errors tend to zero. In addition, a new nonlinear trajectory tracking control law based on trapezoidal approach has been proposed.

The proposed controllers are easy to implement, making it suitable for implementation in low-profile processors. In addition, the control inputs are the linear and angular velocities, common at the most commercial robots. It provides an appropriate value for robot velocity commands, avoiding saturation values of control signals, while keeping a good performance of the control system. In comparison with the previous published control law,[10] the method proposed here, do not need to perform any optimization to calculate the control actions in each sampling period. Finally, the proof of convergence to zero of the tracking errors has been included.

Acknowledgements

This work was partially funded by the Consejo Nacional de Investigaciones Científicas y Técnicas (CONICET – National Council for Scientific Research), Argentina, the Escuela Politécnica Nacional del Ecuador (Facultad de Ingeniería Eléctrica y Electrónica), and the Secretaría Nacional de Educación Superior, Ciencia y Tecnología (SENESCYT) through Prometeo Programm.

References

1. G. Scaglia, L. Q. Montoya, V. Mut and F. di Sciascio, "Numerical methods based controller design for mobile robots," *Robotica* **27**(2), 269–279 (2009).
2. V. Andaluz, F. Roberti, J. M. Toibero and R. Carelli, "Adaptive unified motion control of mobile manipulators," *Control Eng. Pract.* **20**(12), 1337–1352 (2012).
3. F. N. Martins, W. C. Celeste, R. Carelli, M. Sarcinelli-Filho and T. F. Bastos-Filho, "An adaptive dynamic controller for autonomous mobile robot trajectory tracking," *Control Eng. Pract.* **16**(11), 1354–1363 (2008).
4. A. Rosales, G. Scaglia, V. Mut and F. Di Sciascio, "Trajectory tracking of mobile robots in dynamic environments-a linear algebra approach," *Robotica* **27**(7), 981–997 (2009).
5. A. Rosales, G. Scaglia, V. Mut and F. Di Sciascio, "Formation control and trajectory tracking of mobile robotic systems - A Linear Algebra approach," *Robotica* **29**(3), 335–349 (2011).
6. M. E. Serrano, G. J. E. Scaglia, S. A. Godoy, V. Mut and O. A. Ortiz, "Trajectory Tracking of Underactuated Surface Vessels: A Linear Algebra Approach," *IEEE Trans. on Control Syst. Technol.* **20**(3), 1103–1111 (2013).
7. T.-C. Lee, K.-T. Song, C.-H. Lee and C.-C. Teng, "Tracking control of unicycle-modeled mobile robots using a saturation feedback controller," *IEEE Trans. Control Syst. Technol.* **9**(2), 305–318 (2001).
8. G. Klančar and I. Škrjanc, "Tracking-error model-based predictive control for mobile robots in real time," *Robot. Auton. Syst.* **55**(6), 460–469 (2007).
9. C. Z. Resende, R. Carelli and M. Sarcinelli-Filho, "A nonlinear trajectory tracking controller for mobile robots with velocity limitation via fuzzy gains," *Control Eng. Pract.* **21**(10), 1302–1309 (2013).
10. M. E. Serrano, G. J. E. Scaglia, F. A. Cheein, V. Mut and O. A. Ortiz, "Trajectory-tracking controller design with constraints in the control signals: A case study in mobile robots," *Robotica* (2014). doi:10.1017/S0263574714001325.
11. G. Scaglia, A. Rosales, L. Quintero, V. Mut and R. Agarwal, "A linear-interpolation-based controller design for trajectory tracking of mobile robots," *Control Eng. Pract.* **18**(3), 318–329 (2010).
12. J. M. Toibero, F. Roberti and R. Carelli, "Stable contour-following control of wheeled mobile robots," *Robotica* **27**(1), 1–12 (2009).
13. L. A. Strang and L. Aleebra, *Its Applications* (Academic Press, New York, 1980).
14. R. W. Brockett, "Asymptotic Stability and Feedback Stabilization," *Proceedings of the Conference Held at Michigan Technological University* (1983) **vol.** 27, pp. 181–208.
15. J. E. Normey-Rico, I. Alcalá, J. Gómez-Ortega and E. F. Camacho, "Mobile robot path tracking using a robust PID controller," *Control Eng. Pract.* **9**(11), 1209–1214 (2001).
16. J. E. Normey-Rico, J. Gómez-Ortega and E. F. Camacho, "A Smith-predictor-based generalised predictive controller for mobile robot path-tracking," *Control Eng. Pract.* **7**(6), 729–740 (1999).
17. P. D. Cha and J. I. Molinder, *Fundamentals of Signals and Systems with CD-ROM: A Building Block Approach* (Cambridge University Press, 2006).
18. K. Marti, *Stochastic Optimization Methods* (Springer, 2008).

https://doi.org/10.1017/S026357471500020X Published online by Cambridge University Press

19. S. A. Roth and P. Batavia, "Evaluating Path Tracker Performance for Outdoor Mobile Robots," *Automation Technology for Off-Road Equipment* (2002).

Appendix

Proof 1 Analysis: If the system behavior is ruled by Eq. (15) and the controller is designed by Eqs. (30), (33), and (35), then $e_n \to 0, n \to \infty$ when trajectory tracking problems are considered and the controller parameters fulfill $0 < k_v < 1$ and $0 < k_w < 1$.

Remark 5: Consider the next geometric progression

$$\begin{aligned} a_1 &= ka_0 \\ a_2 &= ka_1 = k^2 a_0 \\ &\vdots \\ a_{n+1} &= ka_n = k^n a_0. \end{aligned}$$

Then, if $0 < k < 1$ and $n \to \infty$ (with n N), then $a_n \to 0$.

The proof of convergence to zero of the tracking errors starts with the variable θ.

Considering the orientation from Eq. (15) and the control action from Eq. (35)

$$\theta_{n+1} = \theta_n + \frac{T_0}{2}\left(W_n + W_{n+1}\right) \tag{A.1}$$

$$W_{n+1} = \frac{2}{T_0}\left(\theta_{ez,n+1} - k_w\left(\theta_{ez,n} - \theta_n\right) - \theta_n\right) - \frac{\theta_{ez,n+1} - \theta_{ez,n}}{T_0}. \tag{A.2}$$

By replacing the control action W_{n+1} given by Eq. (A.2) in Eq. (A.1) and the Euler's approximation of W_n, the following expression is found:

$$\theta_{n+1} = \theta_n + \frac{T_0}{2}\left(\frac{\theta_{n+1} - \theta_n}{T_0} + \frac{2}{T_0}\left(\theta_{ez,n+1} - k_w\left(\theta_{ez,n} - \theta_n\right) - \theta_n\right) - \frac{\theta_{ez,n+1} - \theta_{ez,n}}{T_0}\right). \tag{A.3}$$

After some simple operations, it yields

$$\theta_{ez,n+1} - \theta_{n+1} - k_w\left(\theta_{ez,n} - \theta_n\right) - \frac{1}{2}\left(\theta_{ez,n+1} - \theta_{n+1}\right) + \frac{1}{2}\left(\theta_{ez,n} - \theta_n\right) = 0. \tag{A.4}$$

In Eq. (A.4) the difference between $\theta_{ez,n}$ and θ_n will be denoted by e_θ and represent the orientation error to the robot reach and follow the reference trajectory. Thus, Eqs. (A.5) and (A.6) results

$$\frac{e_{\theta,n+1}}{2} - \left(k_w - \frac{1}{2}\right)e_{\theta,n} = 0 \tag{A.5}$$

$$e_{\theta,n+1} - (2k_w - 1)\, e_{\theta,n} = 0. \tag{A.6}$$

Thus, such that the error in Eq. (A.6) tends asymptotically to zero

$$(2k_w - 1) < 1 \Rightarrow 0 < k_w < 1. \tag{A.7}$$

Then, if $0 < k_w < 1$ and $n \to \infty$ (with n N), then $e_{\theta,n+1} \to 0$ (see Remark 5).

Now, the convergence analysis of e_x and e_y is developed below. From the corresponding equation of the system (15)

$$x_{n+1} = x_n + \frac{T_0}{2}\left(V_n \cos\theta_n + V_{n+1}\cos\theta_{n+1}\right). \tag{A.8}$$

https://doi.org/10.1017/S026357471500020X Published online by Cambridge University Press

By using the Taylor interpolation rule, the functions $\cos\theta_{n+1}$ can be expressed as

$$\cos\theta_{n+1} = \cos\theta_{ez,n+1} - \sin\underbrace{\left(\theta_{ez,n+1} + \lambda\left(\theta_{ez,n+1} - \theta_n\right)\right)}_{\theta_{\lambda,n}}\underbrace{\left(\theta_{n+1} - \theta_{ez,n+1}\right)}_{-e_{\theta,n+1}}; 0 < \lambda < 1 \tag{A.9}$$

where ,$\theta_{\lambda,n}$ is an interpolation point between θ_{n+1} and $\theta_{ez,n+1}$. Thus, Eq. (A.8) will be

$$x_{n+1} = x_n + \frac{T_0}{2}\left(V_n\cos\theta_n + V_{n+1}\cos\theta_{ez,n+1} + \underbrace{V_{n+1}\sin\theta_{\lambda,n}}_{f_{\lambda,n}}e_{\theta,n+1}\right). \tag{A.10}$$

Then, considering the control action V_{n+1} in Eq. (35) and multiplying by $\cos\theta_{ez,n+1}$

$$\begin{aligned} V_{n+1}\cos\theta_{ez,n+1} = &\left(\left(\frac{2}{T_0}\Delta_x - V_{\text{ref},n}\cos\theta_{\text{ref},n}\right)\cos\theta_{ez,n+1}\right. \\ &\left. + \left(\frac{2}{T_0}\Delta_y - V_{\text{ref},n}\sin\theta_{\text{ref},n}\right)\sin\theta_{ez,n+1}\right)\cos\theta_{ez,n+1}. \end{aligned} \tag{A.11}$$

From Eq. (30)

$$\frac{2}{T_0}\Delta_y - V_{\text{ref},n}\sin\theta_{\text{ref},n} = \left(\frac{2}{T_0}\Delta_x - V_{\text{ref},n}\cos\theta_{\text{ref},n}\right)\frac{\sin\theta_{ez,n+1}}{\cos\theta_{ez,n+1}}. \tag{A.12}$$

Considering Eqs. (A.11) and (A.12), after some simple operations, it yields

$$V_{n+1}\cos\theta_{ez,n+1} = \left(\frac{2}{T_0}\Delta_x - V_{\text{ref},n}\cos\theta_{\text{ref},n}\right)\cos^2\theta_{ez,n+1} + \left(\frac{2}{T_0}\Delta_x - V_{\text{ref},n}\cos\theta_{\text{ref},n}\right)\sin^2\theta_{ez,n+1} \tag{A.13}$$

leading to

$$V_{n+1}\cos\theta_{ez,n+1} = \left(\frac{2}{T_0}\Delta_x - V_{\text{ref},n}\cos\theta_{\text{ref},n}\right). \tag{A.14}$$

Taking into account Eqs. (A.10) and (A.14), it can be shown that

$$x_{n+1} = x_n + \frac{T_0}{2}\left(V_n\cos\theta_n + \left(\frac{2}{T_0}\Delta_x - V_{\text{ref},n}\cos\theta_{\text{ref},n}\right) + \underbrace{V_{n+1}\sin\theta_{\lambda,n}}_{f_{\lambda,n}}e_{\theta,n+1}\right). \tag{A.15}$$

Next, the following replacements are considered:

$$V_n\cos\theta_n = \frac{x_{n+1} - x_n}{T_0} \text{ and } V_{\text{ref},n}\cos\theta_{\text{ref},n} = \frac{x_{\text{ref},n+1} - x_{\text{ref},n}}{T_0}. \tag{A.16}$$

According to Eq. (A.15)

$$x_{\text{ref},n+1} - x_{n+1} - k_v\left(x_{\text{ref},n} - x_n\right) + \frac{x_{n+1}}{2} - \frac{x_{\text{ref},n+1}}{2} - \frac{x_n}{2} + \frac{x_{\text{ref},n}}{2} + \frac{T_0}{2}f_{\lambda,n}e_{\theta,n+1} = 0. \tag{A.17}$$

Thence

$$e_{x,n+1} - k_v e_{x,n} - \frac{e_{x,n+1}}{2} + \frac{e_{x,n}}{2} + \frac{T_0}{2}f_{\lambda,n}e_{\theta,n+1} = 0 \tag{A.18}$$

https://doi.org/10.1017/S026357471500020X Published online by Cambridge University Press

$$\frac{e_{x,n+1}}{2} - e_{x,n}\left(k_v - \frac{1}{2}\right) + \frac{T_0}{2} f_{\lambda,n} e_{\theta,n+1} = 0 \tag{A.19}$$

$$e_{x,n+1} - e_{x,n}\left(2k_v - 1\right) + T_0 f_{\lambda,n} e_{\theta,n+1} = 0. \tag{A.20}$$

Now, the same reasoning is applied to the y-coordinate.

From the corresponding equation of the system (15)

$$y_{n+1} = y_n + \frac{T_0}{2}\left(V_n \sin\theta_n + V_{n+1}\sin\theta_{n+1}\right). \tag{A.21}$$

By using the Taylor interpolation rule, the functions $\sin\theta_{n+1}$ can be expressed as

$$\sin\theta_{n+1} = \sin\theta_{ez,n+1} + \cos\underbrace{\left(\theta_{ez,n+1} + \psi\left(\theta_{ez,n+1} - \theta_n\right)\right)}_{\theta_{\psi,n}}\underbrace{\left(\theta_{n+1} - \theta_{ez,n+1}\right)}_{-e_{\theta,n+1}}; 0 < \psi < 1 \tag{A.22}$$

where $\theta_{\psi,n}$ is an interpolation point between θ_{n+1} and $\theta_{ez,n+1}$. Thus, Eq. (A.21) will be:

$$y_{n+1} = y_n + \frac{T_0}{2}\left(V_n \sin\theta_n + V_{n+1}\sin\theta_{ez,n+1} - \underbrace{V_{n+1}\cos\theta_{\psi,n}}_{f_{\psi,n}} e_{\theta,n+1}\right). \tag{A.23}$$

Then, considering the control action V_{n+1} in Eq. (35) and multiplying by $\sin\theta_{ez,n+1}$

$$\begin{aligned} V_{n+1}\sin\theta_{ez,n+1} = &\left(\left(\frac{2}{T_0}\Delta_x - V_{\mathrm{ref},n}\cos\theta_{\mathrm{ref},n}\right)\cos\theta_{ez,n+1}\right. \\ &\left. + \left(\frac{2}{T_0}\Delta_y - V_{\mathrm{ref},n}\sin\theta_{\mathrm{ref},n}\right)\sin\theta_{ez,n+1}\right)\sin\theta_{ez,n+1}. \end{aligned} \tag{A.24}$$

From Eq. (30)

$$\frac{2}{T_0}\Delta_x - V_{\mathrm{ref},n}\cos\theta_{\mathrm{ref},n} = \left(\frac{2}{T_0}\Delta_y - V_{\mathrm{ref},n}\sin\theta_{\mathrm{ref},n}\right)\frac{\cos\theta_{ez,n+1}}{\sin\theta_{ez,n+1}}. \tag{A.25}$$

According to Eqs. (A.24) and (A.25), after some simple operations

$$V_{n+1}\sin\theta_{ez,n+1} = \left(\frac{2}{T_0}\Delta_y - V_{\mathrm{ref},n}\sin\theta_{\mathrm{ref},n}\right)\cos^2\theta_{ez,n+1} + \left(\frac{2}{T_0}\Delta_y - V_{\mathrm{ref},n}\sin\theta_{\mathrm{ref},n}\right)\sin^2\theta_{ez,n+1} \tag{A.26}$$

$$V_{n+1}\sin\theta_{ez,n+1} = \left(\frac{2}{T_0}\Delta_y - V_{\mathrm{ref},n}\sin\theta_{\mathrm{ref},n}\right). \tag{A.27}$$

Taking into account Eqs. (A.23) and (A.27), it can be shown that

$$y_{n+1} = y_n + \frac{T_0}{2}\left(V_n\sin\theta_n + \left(\frac{2}{T_0}\Delta_y - V_{\mathrm{ref},n}\sin\theta_{\mathrm{ref},n}\right) - f_{\psi,n}e_{\theta,n+1}\right). \tag{A.28}$$

Next, the following replacements are considered:

$$V_n\sin\theta_n = \frac{y_{n+1} - y_n}{T_0} \text{ and } V_{\mathrm{ref},n}\sin\theta_{\mathrm{ref},n} = \frac{y_{\mathrm{ref},n+1} - y_{\mathrm{ref},n}}{T_0}. \tag{A.29}$$

https://doi.org/10.1017/S026357471500020X Published online by Cambridge University Press

Considering Eq. (A.29) and taking into account Eq. (A.28)

$$y_{\text{ref},n+1} - y_{n+1} - k_v\left(y_{\text{ref},n} - y_n\right) + \frac{y_{n+1}}{2} - \frac{y_{\text{ref},n+1}}{2} - \frac{y_n}{2} + \frac{y_{\text{ref},n}}{2} - \frac{T_0}{2} f_{\psi,n} e_{\theta,n+1} = 0. \quad \text{(A.30)}$$

Thence

$$e_{y,n+1} - k_v e_{y,n} - \frac{e_{y,n+1}}{2} + \frac{e_{y,n}}{2} - \frac{T_0}{2} f_{\psi,n} e_{\theta,n+1} = 0 \quad \text{(A.31)}$$

$$\frac{e_{y,n+1}}{2} - e_{y,n}\left(k_v - \frac{1}{2}\right) - \frac{T_0}{2} f_{\psi,n} e_{\theta,n+1} = 0 \quad \text{(A.32)}$$

leading to

$$e_{y,n+1} - e_{y,n}\left(2k_v - 1\right) - T_0 f_{\psi,n} e_{\theta,n+1} = 0. \quad \text{(A.33)}$$

Considering Eqs. (A.20) and (A.33) and taking into account that

$$e_{\theta,n+1} = \left(2k_w - 1\right) e_{\theta,n} e_{\theta,n+1} \to 0, n \to \infty$$

it yields, in compact form to

$$\begin{bmatrix} e_{x,n+1} \\ e_{y,n+1} \end{bmatrix} = \begin{bmatrix} 2k_v - 1 & 0 \\ 0 & 2k_v - 1 \end{bmatrix} \begin{bmatrix} e_{x,n} \\ e_{y,n} \end{bmatrix} + \underbrace{\begin{bmatrix} -T_0 f_{\lambda,n} \\ T_0 f_{\psi,n} \end{bmatrix} e_{\theta,n+1}}_{\text{bounded nonlinearity} \to 0} \quad \text{(A.34)}$$

Thus, for $0 < k_v < 1$, the error in Eq. (A.34) tends asymptotically to zero.

Remark 6: The Eq. (A.34) is a linear system with a nonlinearity that tends to zero. It can be shown that the nonlinearity is bounded in the same manner as shown for other functions in ref. [11]. If $0 < k_v < 1$, then $e_{x,n} \to 0$ and $e_{y,n} \to 0$, when $n \to \infty$ (Appendix A Eqs. (A31), (A35)–(A41))[11].

https://doi.org/10.1017/S026357471500020X Published online by Cambridge University Press